

# Preparation and electrochemical performance of polyaniline-based carbon nanotubes as electrode material for supercapacitor

Miaomiao Yang, Bin Cheng, Huaihe Song\*, Xiaohong Chen

State Key Laboratory of Chemical Resource Engineering, Beijing University of Chemical Technology, Beijing 100029, PR China

## ARTICLE INFO

### Article history:

Received 3 May 2010

Received in revised form 22 June 2010

Accepted 26 June 2010

Available online 19 July 2010

### Keywords:

Polyaniline

Carbon nanotubes

Electrochemical supercapacitor

Nitrogen-doping

Cyclic voltammetry

## ABSTRACT

Nitrogen-containing carbon nanotubes (CNTs) with open end and low specific surface area were prepared via the carbonization of polyaniline (PANI) nanotubes synthesized by a rapidly mixed reaction. On the basis of analyzing the morphologies and structures of the original and carbonized PANI nanotubes, the electrochemical properties of PANI-based CNTs obtained at different temperatures as electrode materials for supercapacitors using 30 wt.% aqueous solution of KOH as electrolyte were investigated by galvanostatic charge/discharge and cyclic voltammetry. It was found that the carbonized PANI nanotubes at 700 °C exhibit high specific capacitance of 163 F g<sup>-1</sup> at a current density of 0.1 A g<sup>-1</sup> and excellent rate capability in KOH solution. Using X-ray photoelectron spectroscopy measurement the nitrogen state and content in PANI-CNTs were analysed, which could play important roles for the enhancement of electrochemical performance. When the appropriate content of nitrogen is present, the presence of pyrrole or pyridone and quaternary nitrogen is beneficial for the improvement of electron mobility and the wettability of electrode.

© 2010 Elsevier Ltd. All rights reserved.

## 1. Introduction

Supercapacitor, which possesses high power density, high cycle efficiency and a long cycle life, has attracted more and more attention owing to its wide range of potential applications, such as hybrid power sources for electric vehicles, digital telecommunication systems and pulse laser technique [1]. According to the mechanism of energy storage, supercapacitor can be divided into two types: one is the electric double-layer capacitor (EDLC), which stores energy through the separation of electronic and ionic charges at the interface between electrode and an electrolyte solution. The other is pseudocapacitor, which has Faradic reactions on the electrode materials [2]. Three types of electrode materials have been investigated for supercapacitor: carbon materials [1], metal oxides, such as RuO<sub>2</sub> and MnO<sub>2</sub> [3] and conducting polymers, such as polyaniline, polythiophene and polypyrrole [3]. Carbon materials are the most important and applicable electrode materials for commercial supercapacitor because of their stability in different solutions, well processability and relatively low cost [4]. Otherwise, it was found that nitrogen-rich carbon materials can also be used as electrode materials for supercapacitors [5–11]. Lota et al. prepared nitrogen-enriched porous carbons as electrodes by pyrolyzing nitrogen-containing polymers and their blends with coal-tar pitch, and pointed out that combining a high surface area

and a ration of the content of nitrogen seems to be a promising way to improve the performance of supercapacitors [12]. They also investigated the nanotube-based composites being rich in nitrogen, and obtained the capacitances of 160, 120 and 55 F g<sup>-1</sup> at 1 mHz, 1 and 10 Hz, respectively [6]. Kawaguchi et al. [13] reported a nitrogen-containing carbonaceous material by pyrolysis of 2,3,6,7-tetracyano-1,4,5,8-tetraazanaphthalene, and discussed the roles of nitrogen for the improvement of specific capacitance. It is believed that the presence of nitrogen changes the electron donor/acceptor properties of graphene layers, thus affects the formation of electric double-layers [14]. Simultaneously, the introduction of nitrogen could produce a pseudo-capacitance besides the electric double-layer capacitance, enhance the wettability in electrode-electrolyte interface, and then improve the capacitance of electrode [13].

Since the first report on carbon nanotubes (CNTs) in 1991, CNTs are of great interest due to their nanometer size, electrical conductivity and mechanical performance [15]. Because of the unique morphology, well-controlled nanostructure, surface functionality and the cyclicity of the power supply, CNTs are regarded as suitable materials for electrodes in supercapacitors and lithium-ion batteries [15–17]. The capacitances of carbon nanotube electrodes for supercapacitors are generally in the range of 40–80 F g<sup>-1</sup> [18]. Because the value depends upon nanotubes' components, morphologies, surfaces and pore structures, it can be enhanced by surface modification or attaching functional groups [4,18]. Modifying these nanotubes by introducing heteroatoms, such as nitrogen, is a known application in electrochemistry [5–7]. Jurewicz et al. [7] modified multi-walled carbon nanotubes containing nitrogen by

\* Corresponding author. Tel.: +86 10 64434916; fax: +86 10 64434916.

E-mail address: [songhh@mail.buct.edu.cn](mailto:songhh@mail.buct.edu.cn) (H. Song).

activation and ammoxidation, and found that the capacitances of modified nanotubes are less than  $100 \text{ F g}^{-1}$ .

Polyaniline (PANI) ranks the most potentially useful conducting polymers because of its facile synthesis, environmental stability, and simple acid/base doping/dedoping chemistry [19]. PANI has been considered as an important material for the application of supercapacitor electrode [20–26]. The composite electrodes of carbon and PANI show a higher capacitance and a good rate capability. Most significantly, by controlling the synthesis conditions, PANIs with various shapes, such as nanowires, nanofibers, nanotubes and hollow spheres, have been produced [27–31]. Correspondingly carbon nanostructures with special morphologies are easily prepared from the PANI nanostructures by maintaining the original shapes of PANIs through high-temperature heat treatment in an inert gas atmosphere. Therefore we can get nitrogen-enriched carbon nanomaterials from PANI nanostructures. From this point of view, PANIs with different morphologies can be considered as appropriate precursors for carbon nanomaterials containing nitrogen, which are favourable for the electrochemical energy storage. The obvious way to link both types of materials is the conversion of conducting polymers into carbonaceous structures.

In this paper, we pay more emphasis on the preparation and electrochemical properties of nitrogen-containing CNTs from PANI nanotubes. As well known, a certain content of nitrogen in carbonaceous materials will enhance the capacitance of electrode materials [10,12,14]. The pyrolysis of PANI at high temperatures is a simple method to prepare nitrogen-enriched carbon materials. Although some papers have introduced the carbonization and structural conversion of polyaniline to carbon materials including carbon nanotubes [32–37], there is no report on the carbonized PANI nanomaterial as electrode for supercapacitor by now.

## 2. Experimental

### 2.1. Synthesis of polyaniline nanotubes

PANI nanotubes have been prepared according to the previous literatures [19,38,39]. The typical process was performed as follows: At first, 3.423 g ammonium persulfate (Shantou Chemical Factory, 98%) as the initiator and 1.09 ml aniline monomer (Tianjin Chemical Reagent Factory, 99.5%) were dissolved in 60 ml de-ionized water, respectively. Then the initiator solution was poured into the monomer solution quickly with vigorous stirring, and maintained in a quiescent state at room temperature for 24 h to get the precipitate. The resulting precipitate was centrifugated, washed and dried to obtain the desired PANI nanotubes.

### 2.2. Carbonization of polyaniline nanotubes

In the carbonization experiment, 1.0 g of PANI placed into an alumina crucible was carbonized in a horizontal furnace under pure nitrogen gas atmosphere according to the following heating procedure. The sample was firstly heated to  $400^\circ\text{C}$  with a heating rate of  $1^\circ\text{C min}^{-1}$ , and maintained for 2 h at this temperature, and then it was increased to the ultimate temperatures of 600, 700, 850, 1000 and  $1100^\circ\text{C}$ , respectively, with a heating rate of  $0.5^\circ\text{C min}^{-1}$ , and keeping for 2 h at the final temperatures. The heated samples were weighed and named as PANI-600, PANI-700, PANI-850, PANI-1000, and PANI-1100, respectively.

### 2.3. Characterization of PANI and carbonized polyaniline nanotubes

The morphologies and structures of as-synthesized and carbonized materials were observed by scanning electron microscope (SEM, Hitachi S-4700) and transmission electron microscope (TEM,

Hitachi H-800). The specific surface areas ( $S_{\text{BET}}$ ) were obtained by Micromeritics ASAP 2020 Instrument from the adsorption data in the relative pressure interval from 0.04 to  $0.2 \text{ P P}_0^{-1}$  using Brunauer–Emmett–Teller (BET) method. The elemental composition (C, H and N) was determined using an elemental analyzer (Flash EA 1112). The chemical composition and state of samples were measured by X-ray photoelectron spectroscopy (XPS) under a pressure lower than  $10^{-7} \text{ Pa}$  with a Thermo ESCALAB 250 instrument. XPS spectra were recorded using monochromatic Al K $\alpha$  (1486.6 eV) X-ray sources with 30 eV pass energy in 0.5 eV step over an area of  $650 \mu\text{m} \times 650 \mu\text{m}$  to the sample. Atomic concentrations were calculated using peak areas of elemental lines after Shirley background subtraction, and taking the sensitivity factors into account, the asymmetry parameters, as well as the measured analyzer transmission function. The sample charging was corrected using the C 1s peak (284.6 eV) as an internal standard. The quantitative analysis was performed with XPSPEAK4 software.

### 2.4. Electrode assembly and measurement

The electrochemical performances of prepared samples were measured with a three-electrode system that was described in previous work of our group [20]. 80 wt.% of resulting samples, 10 wt.% of polytetrafluoroethylene (PTFE) and 10 wt.% of acetylene black were mixed together to press into the graphite sheet as the working electrode for supercapacitor. The counter and reference electrodes were Platinum foil and Hg/HgO electrode, respectively. The electrolyte was 30 wt.% KOH aqueous solution. The capacitance properties were studied by galvanostatic charge/discharge and cyclic voltammetry (CV) tests. The galvanostatic charge/discharge was carried out by a Program Testing System (produced by China-Land Com. Ltd., China) with the voltage range from 0.9 to 0.01 V. The cyclic voltammetry was taken with a CHI660B electrochemical working station. The sweep voltage ranged from  $-0.85$  to  $0.01 \text{ V}$  in cyclic voltametric measurements.

## 3. Results and discussion

### 3.1. Morphology and structure of polyaniline nanotubes and carbonized PANI nanotubes

The morphologies of pristine PANI were observed by SEM and TEM, and their images are shown in Fig. 1(a)–(d). As seen in Fig. 1, the prepared PANI is nanotube in morphology with rough surface, which is confirmed by TEM observation. The length of PANI nanotubes is between 1 and  $3 \mu\text{m}$ , and diameters range from 100 to 200 nm. PANI nanotubes cross each other, some inner paths are joined together and each end of tubes is open. The wall thickness of tubes is between 65 and 75 nm. The formation of PANI nanotubes has been analyzed in previous reports [31,39]. Briefly, in the primary stage, nano-sized oligomer crystallites were formed as starting template for the nucleation of PANI nanotubes. The further growth of nanotubes depended on the self-organization of phenazine units.

In order to get nitrogen-containing carbon nanotubes, the prepared PANI nanotubes were heated in  $\text{N}_2$  gas atmosphere at different temperatures from 600 to  $1100^\circ\text{C}$ . During the high-temperature treatment, condensation and polymerization take place with the escape of hydrogen and nitrogen atoms, remaining the carbon skeleton. With increasing temperature, the non-carbon atoms lost more, and the carbon skeleton would gradually shrink. Fig. 2 displays the morphologies of the heated PANI at different temperatures. As seen in Fig. 2, the shape generally maintains well after heat treatment and some carbon nanotubes are destroyed and broken into short tubes at higher temperature. The surface of the carbonized PANI becomes smooth relatively. The TEM images effec-

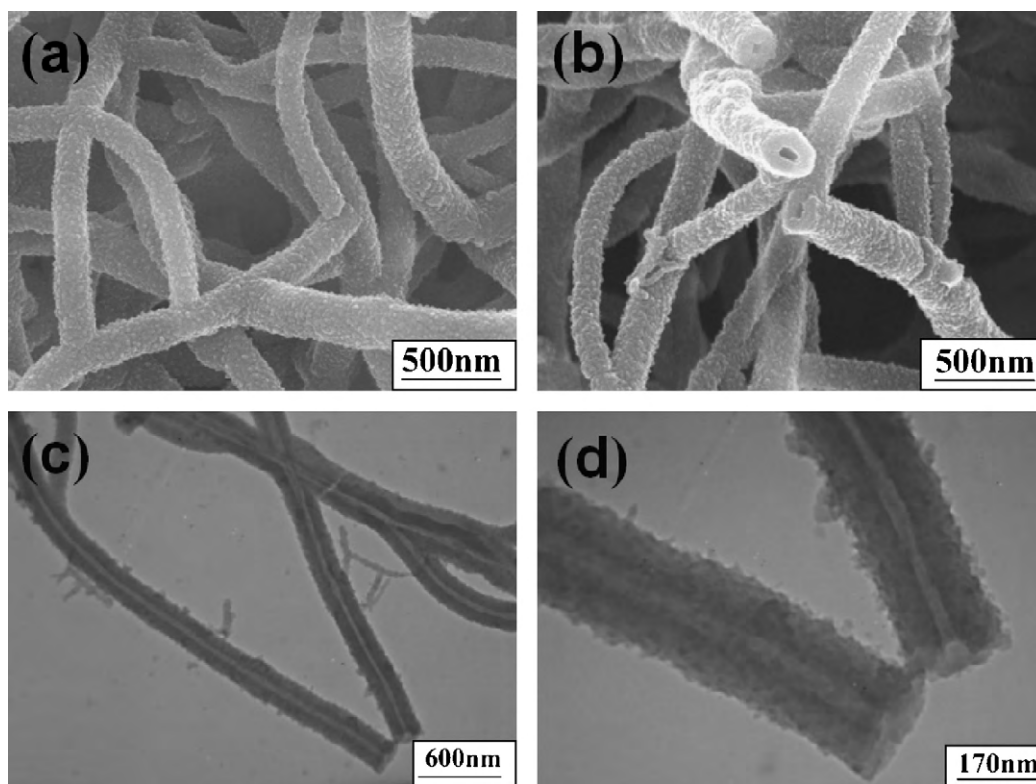


**Fig. 1.** SEM (a and b) and TEM (c and d) images of pristine polyaniline nanotubes.

tively confirm the hollow tubular structure of the carbonized PANI. We can observe each end of tubes is open. The PANI-700 CNTs show the length of 1–2  $\mu\text{m}$  and diameter of 150–170 nm, slightly smaller than that of the pristine PANI nanotubes.

### 3.2. Chemical structure of PANI carbon nanotubes

Elemental analysis and X-ray photoelectron spectroscopy (XPS) were used to measure the elemental composition of carbonized

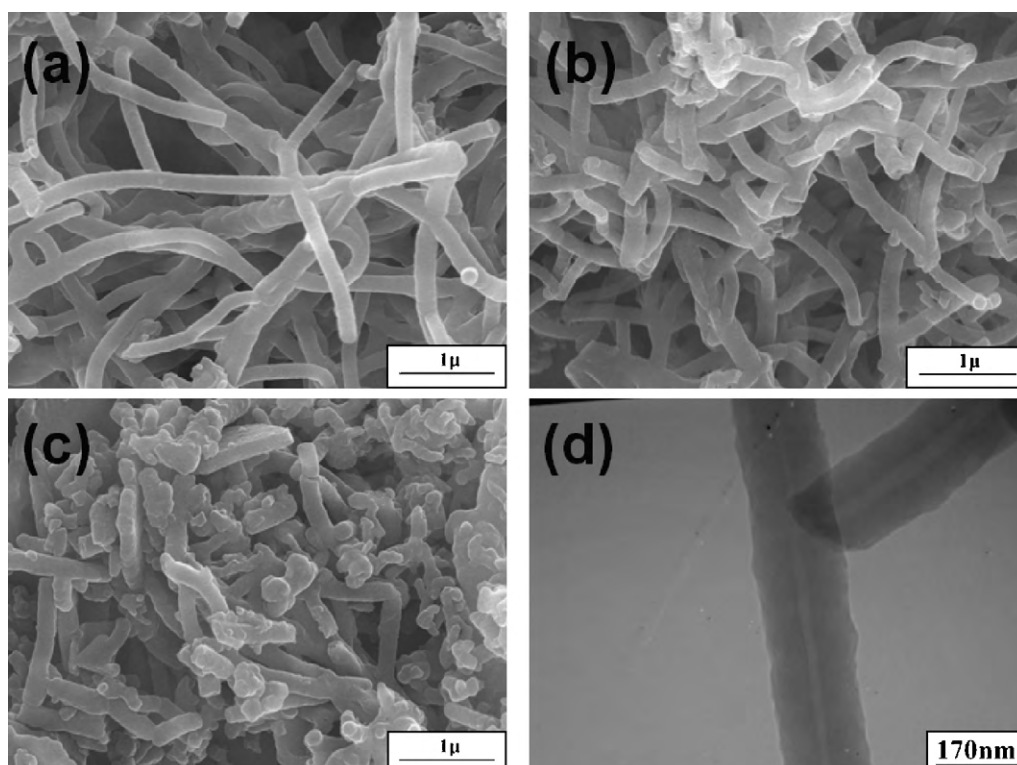


**Fig. 2.** SEM and TEM images of carbonized polyaniline nanotubes at different temperatures (SEM: (a) 600 °C, (b) 700 °C, and (c) 850 °C; TEM: (d) 700 °C).

**Table 1**

The mass loss of PANI carbonized at different temperatures, the elemental composition and the atomic ratio obtained from XPS.

T (°C)	Element content from XPS (at.%)			Mass loss (wt.%)	Elemental composition			
	C	N	O		% C	% H	% N	Difference
600	84.8	9.3	5.9	40.2	82.45	2.21	13.23	2.11
700	87.2	7.4	5.4	46.7	82.8	1.53	10.88	4.79
850	88.9	6.6	4.6	48.3	89.06	1.17	7.95	1.82
1000	92.4	3.1	4.5	50.1	–	–	–	–
1100	93.6	3.1	3.2	52.9	–	–	–	–

samples. All the data are presented in Table 1. Survey XPS spectra of carbonized samples at different temperatures are displayed in Fig. 3. The mass loss of carbonization in Table 1 is calculated based on the weight of previous and carbonized PANI. It can be found that with the temperature increasing from 600 to 1100 °C, the mass loss increases correspondingly. According to the data of elemental analysis, we find that there is a steady decrease in nitrogen and hydrogen contents, and an increase in carbon as the temperature increased, that is consistent with the previous report [32]. The difference between the data of elemental analysis and XPS is caused by different test philosophy. However, the variation tendency of elemental content is the same, i.e., with the temperature increasing from 600 to 1100 °C, the content of carbon goes up. It can be found that the content of oxygen is relatively low compared to that of C and N with the temperature increasing from 600 to 850 °C. The result of above is consistent with elemental analysis.

### 3.3. Electrochemical properties of PANI-based carbon nanotubes

To investigate the electrochemical performance of carbonized PANI nanotubes as electrode material for supercapacitor, galvanostatic charge/discharge cycling measurement was performed in KOH solution. The calculated specific capacitances that are stable after 10 time cycles at every current density are summarized in Fig. 4. Although the PANI-based carbon nanotubes possess low specific surface areas, PANI-700 and PANI-850 electrodes exhibit high capacities of 163 and 110 F g<sup>-1</sup>, respectively, which are higher than that of the pure PANI [20]. As a whole rule, the specific capacitances decrease with the increase of carbonized temperature from 700 to 1100 °C, which could be related with the change of specific surface areas (in Table 2) and the decrease of total polar functional groups [40] as well as the elemental composition. PANI-600 is an exceptional example. Although the specific capacitance of PANI-600 is similar to that of PANI-850 at low current density, it fades fast with the increase of current density, which could be ascribed to the higher polar functional group content and the unstable carbon

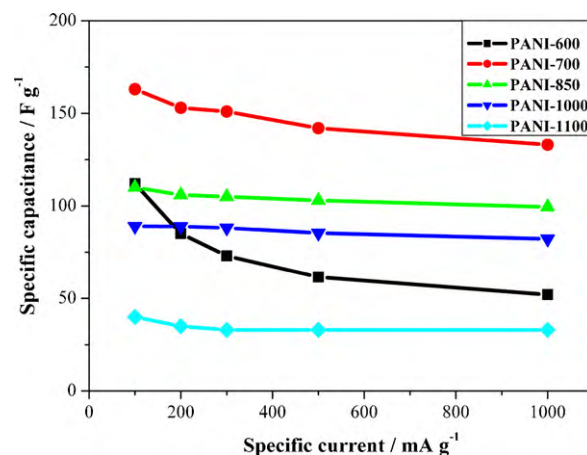


Fig. 4. The specific capacitances of carbonized PANI nanotubes via different heat treatment temperatures at various specific currents in KOH solution.

skeleton formed at the low temperature carbonization. PANI-700 has the highest capacitance in these samples. At a current density of 1 A g<sup>-1</sup> the specific capacitance of PANI-700 is as high as 133 F g<sup>-1</sup>, which is about 82% of the specific capacitance at the current density of 0.1 A g<sup>-1</sup>, implying the high rate capability. Compared with the common activated carbons [1,41], PANI carbon nanotubes possess lower specific surface areas, but higher capacities, which could be related with the chemical state and the content of nitrogen in carbonized PANI samples [10,11,13,14].

The stable charge-discharge cycling curve of carbonized PANI at 700 °C is presented in Fig. 5. The curve is not a perfect triangular shape, indicating a small pseudo-capacitance besides the electric double layer capacitance, which would be caused by the chemical state of nitrogen in PANI-700. Cyclic voltammetry measurements were carried out within the potential range of -0.85 to 0.01 V to analyze the electrochemical behavior of supercapacitor.

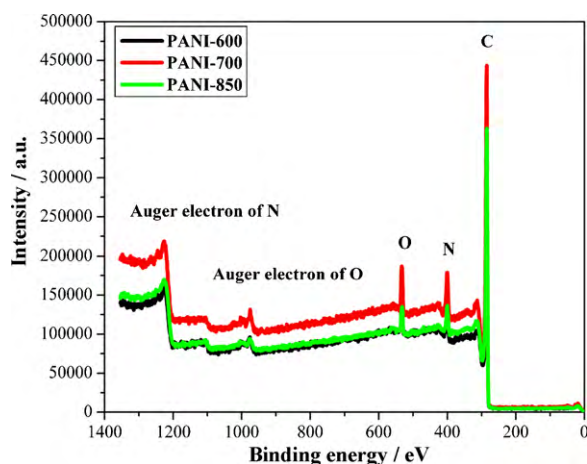


Fig. 3. Survey XPS spectra of carbonized samples at different temperatures.

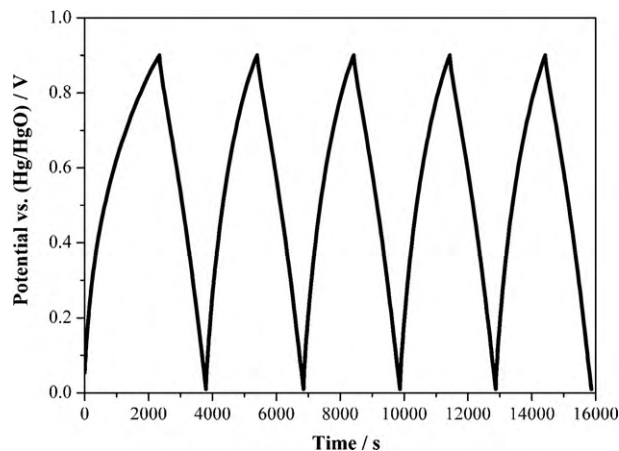
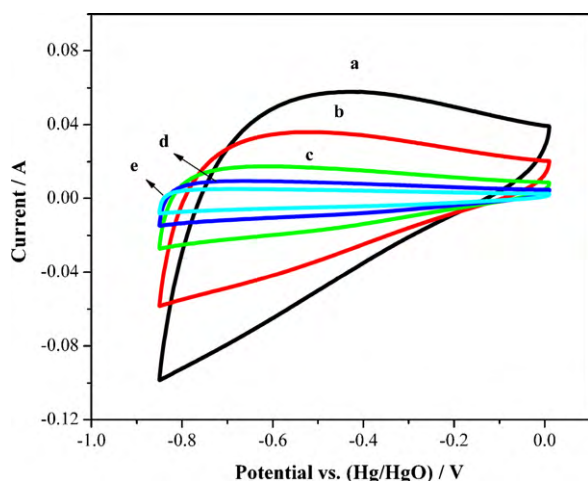


Fig. 5. Galvanostatic charge/discharge cycling curves of PANI-700 electrode in KOH solution.





**Fig. 6.** Cyclic voltammograms of PANI-700 at different sweep rates in aqueous solution of KOH ((a) 0.01 mV s<sup>-1</sup>; (b) 100 mV s<sup>-1</sup>; (c) 50 mV s<sup>-1</sup>; (d) 20 mV s<sup>-1</sup>; (e) 10 mV s<sup>-1</sup>; and (f) 5 mV s<sup>-1</sup>).

Fig. 6 gives the cyclic voltammogram of PANI-700 electrode at different sweep rates. Although the voltammograms are not square and the slopes are present, there is no obvious redox information which is in accordance with the previous report [11], in which the presence of pseudo-capacitance in electrode was confirmed in basic electrolyte, but the mechanism remains unclear. Kawaguchi et al. [13] think that an asymmetrical rectangle of the CV curve is due to the reversible pseudo-faradaic reaction. Hulicova et al. [42] think that this slope is related to the pseudocapacitive properties of carbonized samples, which should be ascribed to the presence of incorporated nitrogen in samples. This statement is in accordance with that deduced from the galvanostatic charge/discharge tests. In addition, we can discover that the quicker the sweep rate is, the bigger the responsive current is, which illustrates that the electrode material has well reversibility.

### 3.4. Effects of nitrogen in PANI-CNTs on the electrochemical performances

The chemical state of nitrogen in PANI carbon nanotubes is investigated by XPS measurement. Table 2 shows the relative quantities of surface nitrogen-containing groups and the specific surface areas of samples. A typical XPS spectrum of N 1s displays in Fig. 7. The chemical state of nitrogen atoms in carbonized samples could be assigned to five types according to previous reports [9,11,12,43,44]. These five types are as following binding energies: 398.4 eV (pyridine-N-6), 400.5 eV (pyrrole or pyridone-N-5), 401 eV (quaternary-N-Q), 402.6 eV (pyridine-N-oxide or ammonia), 405.5 eV (chemisorbed nitrogen oxides-N-Ox). As seen in Table 2, the types of nitrogen in samples and the  $S_{\text{BET}}$  are influenced by the heat treatment temperature. As the temperature increasing from 600 to 850 °C, the specific surface areas decrease from 253.6

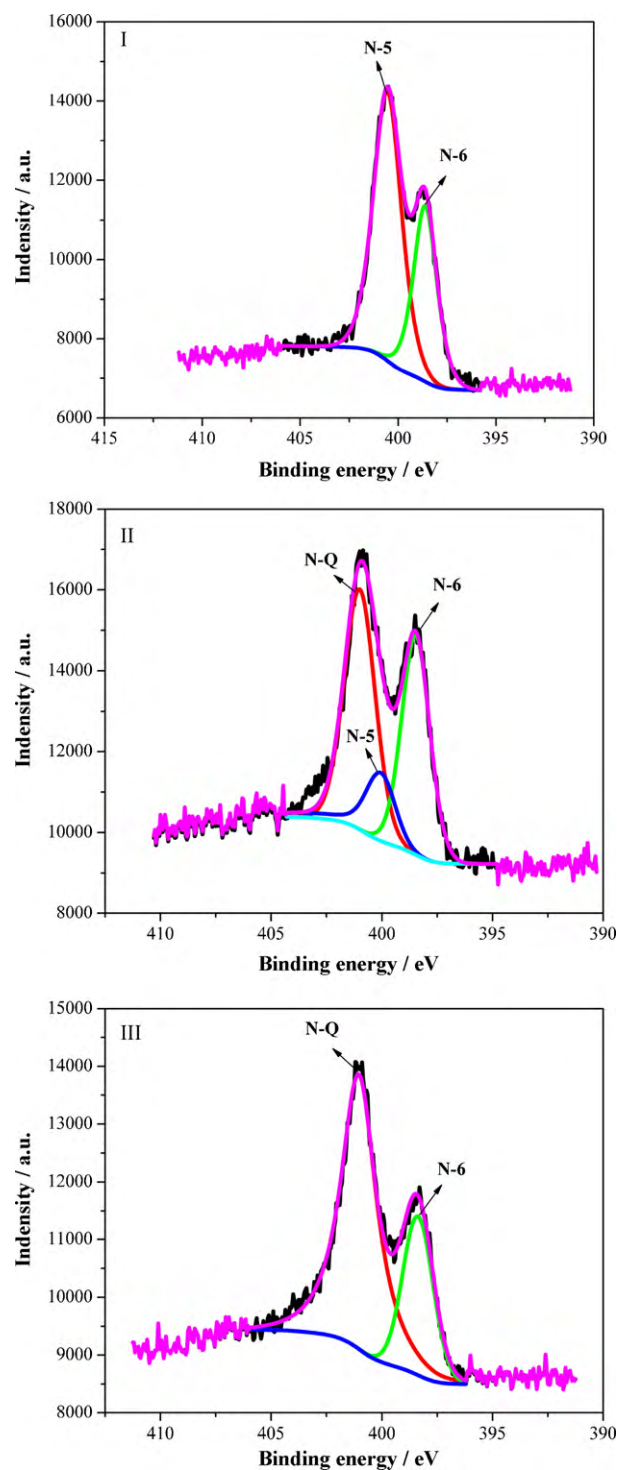


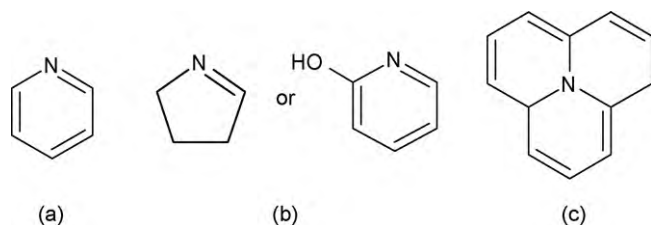
**Fig. 7.** XPS spectra of N 1s of samples: (I) PANI-600; (II) PANI-700 and (III) PANI-850.

**Table 2**

The content of nitrogen species to N 1s peak (%) and  $S_{\text{BET}}$  of the carbonized PANI nanotubes.

Sample (m <sup>2</sup> g <sup>-1</sup> )	Content of nitrogen species from XPS (%)			$S_{\text{BET}}$
	398.4 (eV) N-6	400.5 (eV) N-5	401 (eV) N-Q	
PANI-600	35.6	64.4	–	253.6
PANI-700	38.3	15.8	45.9	46.4
PANI-850	29.4	–	70.6	21.3
PANI-1000	14.9	–	85.1	–
PANI-1100	19.8	–	80.2	–

to 21.3 m<sup>2</sup> g<sup>-1</sup>. The chemical state of nitrogen is complex with different heat temperatures. There are total three types of nitrogen in carbonized products: one at 398.4 eV is attributed to the pyridine (N-6), which is at the edge of graphene layers in six-membered rings [11]; the other one at 400.5 eV belongs to the pyrrole or pyridone (N-5), which is in five-member rings or combined with oxidized form [43]; the last one at about 401 eV is the quaternary (N-Q), the nitrogen atom of which is in a “valley” position [45]. These types of nitrogen groups are presented in Scheme 1. According to Table 2, we can see that all of the samples possess



**Scheme 1.** Types of nitrogen groups: (a) pyridine, (b) pyrrole or pyridone, and (c) quaternary.

N-6. In addition, PANI-600 has N-5, and PANI-850, PANI-1000 and PANI-1100 have N-Q. Only PANI-700 possesses all these types of nitrogen. It was reported that N-6 species can be formed above the temperature of 400 °C, and N-5 will be formed at higher temperature [11,45]. We surmise that with the temperature increasing from 600 to 1100 °C, the state of nitrogen in samples has changed from N-5 to N-Q. At higher temperature, the chemical bond of N-5 is easily broken, and the new C–N or N–Q bond forms. The content and state of nitrogen in samples will affect intensively the capacitive performance.

The insertion of nitrogen atoms into graphene layers can change values of  $E_{\text{HOMO}}$  and  $E_{\text{LUMO}}$  in order to reduce the band gap, thus increase electron mobility and lower the electron work function at the carbon/liquid interface in comparison to pure carbon [44]. There is a conclusion [46–48] that the capacitive behavior is dominated by the electron mobility of the sample. The potential in the double layer is shared between the solvent layer and the space-charge layer, so the capacitance of the sample is provided by these two aspects. Based on this view, increased mobility of electrons in the sample would result in a larger space charge capacitance. Among these samples N-5 and N-Q have electron donor tendency, so their specific capacitances are higher than that of pure PANI. However, PANI-1000 and PANI-1100 possessing low content of nitrogen have relatively low specific capacitances, so we think the appropriate content of nitrogen is a precondition for improving the specific capacitance. PANI-600 and PANI-850 are enriched in N-5 and N-Q, respectively, however PANI-700 is enriched in both of these structures. It is reasonable to believe that possessing both of these structures can endow PANI-700 the highest specific capacitance. In Scheme 1 we can find obviously that N-5 and N-Q have a great difference, in which the former occupies a “top” N position, and the later is in a “valley” N position. According to the report [6], the later one shows stronger donor electron character. Quaternary nitrogen is the most appropriate position affecting the carbon electronic structure in order to lower an energy gap between lowest unoccupied molecular orbital and the highest occupied molecular orbital. So the specific capacitance of PANI-850 possessing quaternary nitrogen is higher than that of PANI-600. Ultimately we conclude that when the appropriate content of nitrogen is present, being both N-5 and N-Q will enhance the capacitance with the following reasons: one is to improve the electron mobility, the other is to enhance the wettability of the electrode to make electrolyte more touch with active materials [13,14].

#### 4. Conclusions

In summary, PANI with the tubular shape was synthesized by a rapidly mixed reaction, and then nitrogen-containing CNTs were prepared through high temperature treatment. The morphologies, structures and electrochemical properties of PANI-based CNTs were investigated. It was found that PANI can maintain the original tubular morphology after heat treatment. The carbon nanotubes possess the diameter of about 100 nm and length of several micrometers with open end and low specific surface area. When

PANI-based CNTs were used as the electrode materials for supercapacitors in KOH solution, they exhibit high specific capacity and good cyclic stability, especially PANI-700 possesses the capacitance of 163 F g<sup>−1</sup> at the current density of 0.1 A g<sup>−1</sup>. The chemical state and content of nitrogen in carbonized PANI nanotubes were investigated by XPS. The reasons why carbonized PANI nanotubes have higher specific capacitance would be ascribed to the presence of pyrrole or pyridone and quaternary nitrogen when the appropriate content of nitrogen is present, which are beneficial for the improvements of electron mobility and the wettability of the electrode.

#### Acknowledgments

This work was supported by the National Natural Science Foundation of China (50872006), State Key Basic Research Program of China (2006CB9326022006), and Foundation of Excellent Doctoral Dissertation of Beijing City (YB20081001001).

#### References

- [1] E. Frackowiak, F. Béguin, *Carbon* 39 (2001) 937.
- [2] R. Kötz, M. Carlen, *Electrochim. Acta* 45 (2000) 2483.
- [3] T.C. Girija, M.V. Sangaranarayanan, *J. Power Sources* 156 (2006) 705.
- [4] A.G. Pandolfo, A.F. Hollenkamp, *J. Power Sources* 157 (2006) 11.
- [5] J.P. Dong, X.M. Qu, L.J. Wang, C.J. Zhao, J.Q. Xu, *Electroanalysis* 20 (2008) 1981.
- [6] G. Lota, K. Lota, E. Frackowiak, *Electrochem. Commun.* 9 (2007) 1828.
- [7] K. Jurewicz, K. Babel, R. Pietrzak, S. Delpoux, H. Wachowska, *Carbon* 44 (2006) 2368.
- [8] K. Jurewicz, R. Pietrzak, P. Nowicki, H. Wachowska, *Electrochim. Acta* 53 (2008) 5469.
- [9] Y.J. Kim, Y. Abe, T. Yanagiura, K.C. Park, M. Shimizu, T. Iwazaki, S. Nakagawa, M. Endo, M.S. Dresselhaus, *Carbon* 45 (2007) 2116.
- [10] W.R. Li, D.H. Chen, Z. Li, Y.F. Shi, Y. Wan, J.J. Huang, J.J. Yang, D.Y. Zhao, Z.Y. Jiang, *Electrochem. Commun.* 9 (2007) 569.
- [11] D.H. Jurcakova, M. Kodama, S. Shiraishi, H. Hatori, Z.H. Zhu, G.Q. Lu, *Adv. Funct. Mater.* 19 (2009) 1.
- [12] G. Lota, B. Grzyb, H. Machnikowska, J. Machnikowski, E. Frackowiak, *Chem. Phys. Lett.* 404 (2005) 53.
- [13] M. Kawaguchi, A. Itoh, S. Yagi, H. Oda, *J. Power Sources* 172 (2007) 481.
- [14] C.X. Zhang, Y.L. Duan, B.L. Xing, L. Zhan, W.M. Qiao, L.C. Ling, *Min. Sci. Technol.* 19 (2009) 295.
- [15] J.H. Chen, W.Z. Li, D.Z. Wang, S.X. Yang, J.G. Wen, Z.F. Ren, *Carbon* 40 (2002) 1193.
- [16] S.B. Yang, H.H. Song, X.H. Chen, A.V. Okotrub, L.G. Bulusheva, *Electrochim. Acta* 52 (2007) 5286.
- [17] S.B. Yang, J.P. Huo, H.H. Song, X.H. Chen, *Electrochim. Acta* 53 (2008) 2238.
- [18] E. Frackowiak, F. Béguin, *Carbon* 40 (2002) 1775.
- [19] D. Li, R.B. Kaner, *J. Am. Soc. Chem.* 128 (2006) 968.
- [20] L.X. Li, H.H. Song, Q.C. Zhang, J.Y. Yao, X.H. Chen, *J. Power Sources* 187 (2009) 268.
- [21] J. Li, J.Z. Zhang, Y.H. Geng, L.X. Wang, X.B. Jing, F.S. Wang, *Synth. Met.* 69 (1995) 245.
- [22] G.C. Xu, W. Wang, X.F. Qu, Y.S. Yin, L. Chu, B.L. He, H.K. Wu, J.R. Fang, Y.S. Bao, L. Liang, *Eur. Polym. J.* 45 (2009) 2701.
- [23] B.C. Kim, J.S. Kwon, J.M. Ko, J.H. Park, C.O. Too, G.G. Wallace, *Synth. Met.* 160 (2010) 94.
- [24] E. Frackowiak, V. Khomenko, K. Jurewicz, K. Lota, F. Béguin, *J. Power Sources* 153 (2006) 413.
- [25] W. Xing, S.P. Zhuo, H.Y. Cui, Z.F. Yan, *Mater. Lett.* 61 (2007) 4627.
- [26] S.W. Woo, K. Dokko, H. Nakano, K. Kanamura, *J. Power Sources* 190 (2009) 596.
- [27] C.R. Martin, *Chem. Mater.* 8 (1996) 1739.
- [28] X.L. Jing, Y.Y. Wang, D. Wu, J.P. Qiang, *Ultrason. Sonochem.* 14 (2007) 75.
- [29] M. Mazur, M. Tagowska, B. Palys, K. Jackowska, *Electrochem. Commun.* 5 (2003) 403.
- [30] B.H. Sung, Y.G. Ko, U.S. Choi, *Colloids Surf. A* 292 (2007) 217.
- [31] J. Stejskal, I. Sapurina, M. Trchová, E.N. Konyushenko, P. Holler, *Polymer* 47 (2006) 8253.
- [32] J.J. Langer, S. Golczak, *Polym. Degrad. Stab.* 92 (2007) 330.
- [33] S. Borrós, E. Muñoz, I. Folch, *J. Chromatogr. A* 837 (1999) 273.
- [34] L. Lin, H.J. Niu, M.L. Zhang, W. Song, Z. Wang, X.D. Bai, *Appl. Surf. Sci.* 254 (2008) 7250.
- [35] K.S. Ho, Y.K. Han, Y.T. Tuan, Y.J. Huang, Y.Z. Wang, T.H. Ho, T.H. Hsieh, J.J. Lin, S.C. Lin, *Synth. Met.* 159 (2009) 1202.
- [36] M. Trchová, P. Matějka, J. Brodinová, A. Kalendová, J. Prokeš, J. Stejskal, *Polym. Degrad. Stab.* 91 (2006) 114.
- [37] M. Trchová, E.N. Konyushenko, J. Stejskal, J. Kovářová, G.C. Marjanović, *Polym. Degrad. Stab.* 94 (2009) 929.

- [38] J.X. Huang, R.B. Kaner, *Angew. Chem.* 116 (2004) 5941.
- [39] N.R. Chiou, L.J. Lee, A.J. Epstein, *Chem. Mater.* 19 (2007) 3589.
- [40] A. Mabuchi, K. Tokumitsu, H. Fujimoto, T. Kasuh, *J. Electrochem. Soc.* 142 (1995) 1041.
- [41] Y. Show, K. Imaizumi, *Diamond Relat. Mater.* 16 (2007) 1154.
- [42] D. Hulicova, J. Yamashita, Y. Soneda, H. Hatori, M. Kodama, *Chem. Mater.* 17 (2005) 1241.
- [43] R. Pietrzak, *Fuel* 88 (2009) 1871.
- [44] W.R. Li, D.H. Chen, Z. Li, Y.F. Shi, Y. Wan, G. Wang, Z.Y. Jiang, D.Y. Zhao, *Carbon* 45 (2007) 1757.
- [45] V.V. Strelko, V.S. Kuts, P.A. Thrower, *Carbon* 38 (2000) 1499.
- [46] M. Hahn, M. Baertschi, O. Barbieri, J.-C. Sauter, R. Kötz, R. Gallay, *Electrochem. Solid-State Lett.* 7 (2004) A33.
- [47] P.W. Ruch, L.J. Hardwick, M. Hahn, A. Foelske, R. Kötz, A. Wolaun, *Carbon* 47 (2009) 38.
- [48] P.W. Ruch, R. Kötz, A. Wokaun, *Electrochim. Acta* 54 (2009) 4451.